J MATER SCI 41 (2006) 1221–1232

Thermo-elastic properties of dense YSZ and porous Ni-ZrO_2 monolithic and isotropic materials

SHIVA GADAG, GANESH SUBBARAYAN*
Purdue University, School of Mechanical Engineering, 585 Purdue Mall, West Lafayette, IN 47907-2088
E-mail: sgadag@purdue.edu
E-mail: ganeshs@purdue.edu

WILLIAM BARKER
ITN Energy Systems, Inc., 8130 Shaffer Parkway, Littleton, CO 80127-4107

Published online: 4 February 2006

Attempts are made to correlate the structure and properties of dense and porous Yittria Stabilized Zirconia to establish optimal thermo-elastic properties for better performance at elevated temperatures. Temperature and compositional dependence of isotropic elastic bulk properties (Young's modulus, Poisson's ratio and Shear and Bulk moduli) are determined using the stiffness constants reported in the literature. Anisotropy of Yittria Stabilized Zirconia increases with composition of Yittria dosage in Zirconia. Optimal composition of 12 mole% Yittria stabilized Zirconia is slightly better than 8 mole% Yittria Stabilized Zirconia based on the improved thermo-elastic properties for better performance at higher temperature (RT-400°C). However 15.5 mole% YSZ seems to be more suitable from the view point of thermo-elastic performance at elevated temperatures (500–800°C). Polycrystalline properties predicted are within 5% error limits of the experimental values for Young's modulus of 12 mole% Yittria Stabilized Zirconia. Numerical prediction of Young's modulus of 12 mole% YSZ for ⟨100⟩ orientation is 362 GPa as compared to experimental value of 370 GPa reported in literature.

1. Introduction

Yittria Stabilized Zirconia (YSZ) is widely used as material for fuel-cell fabrication either by tape casting or sol-gel techniques as an alternative source for power generation. Thin membranes made of dense YSZ often constitute electrolyte material whereas porous NiO/YSZ forms the anode material for the planar design of solid oxide fuel cell. A various types of design strategies are utilized by various research groups [1–7] to develop the optimum alternative source of power by developing fuel-cell batteries for use in automobile or telecommunication industries. The success of design and developments of such solid oxide fuel-cell power by and large depends on well-defined thermal, elastic and plastic properties of the materials varying with temperature. A major stumbling block in the fuel-cell designs using Yittria Stabilized Zirconia materials is the lack of temperature dependant thermo-physical, elastic and plastic properties of dense (YSZ) and porous (Ni/YSZ) materials. A purpose of this paper is to compute the elastic properties viz, elastic moduli, Young's E, Shear -G, Bulk - K and Poisson's ratio, ν of dense YSZ and porous Ni-YSZ materials as a function of temperature and composition of Yittria doped to stabilize the cubic crystal structure of the ZrO_2. The elastic properties of isotropic single crystal or cubic polycrystalline structure of YSZ are calculated here using the elastic stiffness constants by computing the compliance matrix coefficients.

The single crystal elastic constants of cubic YSZ were determined at room temperature from various techniques viz. ultrasonic wave measurements for 8 and 12 mole% Yittria by Pace *et al.* [8], classic vibration by Raleigh's method for 8.8 mole% Yittria by Buckley *et al.* [9] and Brillouin scattering of light between 8 and 20 mole% Yittria by Aleksandrov *et al.* (references: [3–5] in) [10]. The single crystal elastic constants by ultrasonic method for 8 mole% Yittria Stabilized Zirconia at room temperature and also for YSZ phase containing 11.1, 12.1, 15.5 and 17.9 mole% Yittria were measured from 20 to 700°C by

*Author to whom all correspondence should be addressed.
0022-2461
DOI: 10.1007/s10853-005-3660-6

Kandil *et al*. [10]. The only high temperature elastic modulus of YSZ reported in the literature is 155 ± 5 GPa at $T = 900°C$ by Seluc *et al*. [4]. The temperature dependant elastic properties are not available for dense YSZ and especially for porous Ni-YSZ materials. Hence attempts are made to compute the temperature dependant elastic as well the thermal properties of dense and porous materials of Yittria Stabilized Zirconia before and after reduction of NiO-YSZ materials.

2. Experimental

The monolithic and multilayer films on Ni-YSZ substrates were commercially prepared by tape-cast technique. The specimens were used to test bending strength of monolithic or multilayers. The specimens were tested in 3-point bending fixture suitably developed for characterization of ceramic materials as per ASTM procedure. The microstructural features and qualitative and quantitative study of various phases, porosity and fractography were performed using JEOL-3 type of SEM. The micro-mechanics involved in flexural failure and its fractographic analysis will be discussed in a separate communication [11].

3. Numerical procedure

The stress-strain relations of linearly elastic isotropic materials are given by Hook's law as per Equation 1:

$$\sigma_i = C_{ij} \cdot \varepsilon_j \tag{1a}$$

and

$$\varepsilon_i = S_{ij} \cdot \sigma_j \tag{1b}$$

Where, elastic constants C_{ij} and S_{ij} are stiffness and compliance constants of tensorial stress and strain vectors respectively.

A reduced form of Voigt matrix notation of stress (σ_{ij}) and strain (ε_{ij}) are represented by Equation 2:

$$\begin{Bmatrix} \sigma_{11} \\ \sigma_{22} \\ \sigma_{33} \\ \sigma_{23} \\ \sigma_{31} \\ \sigma_{12} \end{Bmatrix} = [C_{ij}] \cdot \begin{Bmatrix} \varepsilon_{11} \\ \varepsilon_{22} \\ \varepsilon_{33} \\ \varepsilon_{23} \\ \varepsilon_{31} \\ \varepsilon_{12} \end{Bmatrix} \tag{2a}$$

and

$$\begin{Bmatrix} \varepsilon_{11} \\ \varepsilon_{22} \\ \varepsilon_{33} \\ \varepsilon_{23} \\ \varepsilon_{31} \\ \varepsilon_{12} \end{Bmatrix} = [S_{ij}] \cdot \begin{Bmatrix} \sigma_{11} \\ \sigma_{22} \\ \sigma_{33} \\ \sigma_{23} \\ \sigma_{31} \\ \sigma_{12} \end{Bmatrix} \tag{2b}$$

Symmetry of cubic crystal structure of ceramics (e.g, 8YSZ, MgO, NaCl) [8, 12] reduces the 6×6 matrix of stiffness (and compliances) coefficients to three independent elastic constants C_{11}, C_{12} and C_{44} and the remaining 33 coefficients are zero [8, 13, 14]. The corresponding three nonzero compliance constants S_{11}, S_{12} and S_{44} in cubic crystal are given by Equations 3a–3c:

$$S_{11} = \frac{(C_{11} + C_{12})}{(C_{11} - C_{12})(C_{11} + 2C_{12})} \tag{3a}$$

$$S_{12} = \frac{-C_{12}}{(C_{11} - C_{12})(C_{11} + 2C_{12})} \tag{3b}$$

and

$$S_{44} = \frac{1}{C_{44}} \tag{3c}$$

Isotropic elastic properties of cubic crystals can be defined in terms of the compliance constants. Isotropic Young's modulus can be defined as an inverse of the compliance coefficients, S_{11} and isotropic shear modulus as half of the inverse of the difference between the compliance constants S_{11} and S_{12}. Isotropic bulk modulus can be defined as one third of the inverse of compliance factor ($S_{11}+2S_{12}$). Three isotropic elastic moduli of the cubic crystals are given by Equation 4a–4c. Poisson's ratio can be defined as the negative ratio of S_{12} to S_{11} as represented by Equation 5. Anisotropy of materials can be defined by a factor (AF) in Equation 6, if it is close to unity the material is said to be highly isotropic. The properties of isotropic cubic materials are independent of the direction of loading. The cubic material is anisotropic if AF>1, elastic properties of the cubic material will then be dependent on the orientation of crystal structure. Young's modulus of a highly anisotropic cubic material depends on direction of external load applied on the material and orientation of the cubic crystal. The directional dependence of elastic modulus of anisotropic cubic material is defined by Cook and Pharr [12] in terms of directional cosine: $R_{\langle hkl \rangle} = [l_1^2 \cdot l_2^2 + l_2^2 \cdot l_3^2 + l_3^2 \cdot l_1^2]$ by Equation 7. Where, l_i are direction cosines of axis of loading with respect to ⟨100⟩ direction for cubic material.

$$E_{\text{Iso}} = \frac{1}{S_{11}} \tag{4a}$$

$$G_{\text{Iso}} = \frac{1}{2(S_{11} - S_{12})} \tag{4b}$$

and

$$K_{\text{Iso}} = \frac{1}{3(S_{11} + 2S_{12})} \tag{4c}$$

$$\nu = -\left(\frac{S_{12}}{S_{11}}\right) \tag{5}$$

$$AF = \frac{2C_{44}}{(C_{11} - C_{12})} \tag{6}$$

$$E_{\langle hkl \rangle} = \frac{1}{(S_{11} - [2\,(S_{11} - S_{12}) - S_{44}] * R_{hkl})} \tag{7}$$

4. Results and discussion

The dense Yittria Stabilized Zirconia (YSZ) tape-cast in the form of thin membranes of 25–50 μm are widely used in the fabrication of electrolytes for fuel-cells consisting of multiple electrode assemblies (MEAs). The porous materials such as YSZ reduced to Ni-ZrO_2 for anode and $La_{(1-x)}Sr_xMnO_3$ or $La_{(1-x)}Sr_xCoO_3$ in definite proportion (40–50%) of YSZ for cathode are commonly used in the fabrication of MEA stacks of the fuel cell. The porosity of the electrodes in composite ceramic MEA stacks helps to transport the ions to increase the electrical conductivity and reduces the thermal diffusivity due to porosity. The mechanical strength of the composite MEA reduces considerably in comparison with individual strength of dense electrolyte or electrodes or Voigt bound modulus based average bending strength using rule of mixture of composite cell materials. Hence, optimum performance of fuel-cell is a compromise between electrical and thermo-mechanical properties of such materials.

4.1. Structure and property correlations

In the following two sections attempt is made to correlate the microstructure features with the thermo-mechanical properties of dense and porous Yittria Stabilized Zirconia (YSZ).

4.1.1. Dense YSZ

The crystal structure of Zirconia doped with 8 mole% or more of Yittria (Y_2O_3) predominantly consists of cubic crystalline structure, which exhibits optimum thermal and electrical conductivity and reasonably good mechanical properties. Typical microstructures obtained by using SEM pictures of dense YSZ and that of sintered and reduced NiO-YSZ along with its back scattered image, are shown in Fig. 1. The micro-structural qualitative features and phase quantification were carried out by scanning the back scattered secondary electron beams. SEM microstructure of fully stabilized dense 8YSZ confirmed cubic structure and reduced Ni-YSZ had porous structure. Occasionally pinhole type of porosity, were found scattered even in the dense material with an average pore size of 0.1–1 μm. The pinhole porosity of the dense material could be due to 3% volume expansion of ZrO_2 during sintering (1200–1400°C) and there by resulting in shrinkage porosity of dense material of 3–5% maximum after subsequent cooling to ambient. Obviously 8 mole% of Y_2O_3 stabilizer dosage in ZrO_2 may be inadequate to avoid the porosity in YSZ even though it could fully stabilize cubic structure. On the contrary, a limited amount of shrinkage porosity in the nearly dense YSZ material might be beneficial to the ionic transportation through the electrolyte. Effect of composition of Yittria doped in ZrO_2 on ionic conductivity in Fig. 2, clearly indicates that a minimum of 8–9 mole% of Yittria Stabilized Zirconia (YSZ) is necessary for fabrication of thin but dense membranes for fuel-cell electrolytes. The ionic conductivity of electrolyte decreases slightly from 15 to 11 mho/meter (ohm-m)$^{-1}$ at 1273°K by increasing Yittria composition from 8 to 12 mole% in YSZ from work of Badwal [15]. The ionic conductivity of 12 mole% YSZ is comparable to that of 8 mole% YSZ at intermediate temperatures (600–770°K). At higher temperatures (900–1111°K) ionic conductivity of 12 mole% YSZ is comparable to that of 3 mole% YSZ [16]. However, interfacial ionic conductivity of typical $A_2B_2O_7$ type of $La_2Zr_2O_7$ compounds formed in composite cathodes (LSM/YSZ) Yittria stabilized Zirconia electrolytes. Interfacial ionic conductivity calculated from the Arrhenius relation (Fig. 2B) is~1.2E-3 S/m at 1273°K.

The lattice parameter, a_0 of Yittria Stabilized Zirconia over a wide range of dosage of Y_2O_3 stabilizer depends on density, ρ of a dense material as per the model of Aleksandrov *et al*. [17] in Equation 8:

$$a_0 = \left[\left(C - \frac{b \cdot M}{(100 + M)}\right) \cdot (1/\rho)\right]^{\frac{1}{3}} \tag{8}$$

(Where, M–mole%Y_2O_3; C and b are material constants for binary system Y_2O_3.ZrO_2 given in reference [17])

At constant molar composition of Yittria, density of Yittria Stabilized Zirconia is inversely proportional to cubic exponent of lattice parameter and hence the lattice constant as per Equation (8). Higher densification of YSZ can be achieved by decreasing lattice parameter with increasing Yittria dosage in Zirconia. This is ultimately governed by maximum packing density of the atoms in cubic structure of YSZ.

At higher temperature Yittria Stabilized Zirconia undergoes thermal expansion inducing thermal strains due to a change in lattice parameter or lattice spacing as per Equation 9a:

$$\varepsilon_{\text{lattice}} = \frac{d_f - d_0}{d_0} \cdot 100 = \frac{a_f - a_0}{a_0} \cdot 100 \tag{9a}$$

and

$$\varepsilon_{\text{thermal}} = \overline{\alpha}_{ysz} \cdot \Delta T \tag{9b}$$

The density of dense YSZ can be accurately measured by Archimedes method to determine the lattice spacing or X-ray diffraction of YSZ can be used to determine lattice parameter and to compute the thermal strains induced in the lattice or vice versa by using Equations 8 and 9.

$$\bar{\alpha}_{\text{ysz}} = (8 + 0.003 \cdot T) \cdot 10^{-6}/^{\circ}C \tag{10}$$

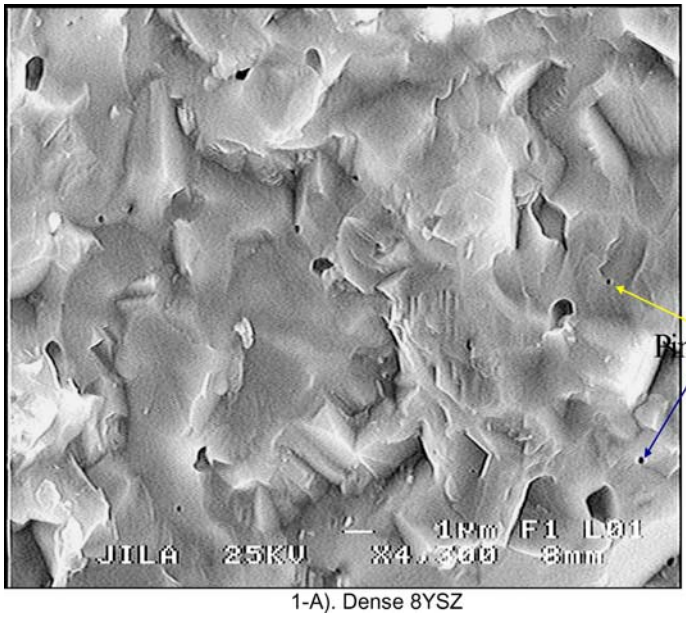

1-A). Dense 8YSZ

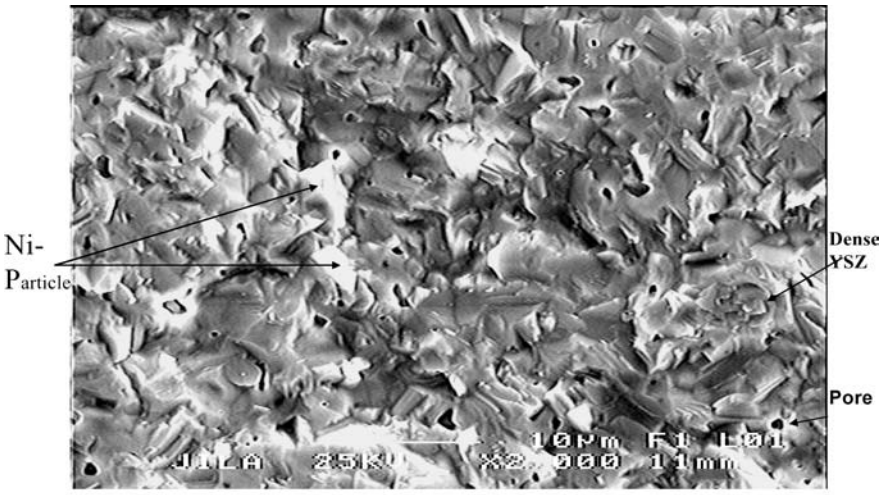

1-B). Porous Ni-YSZ

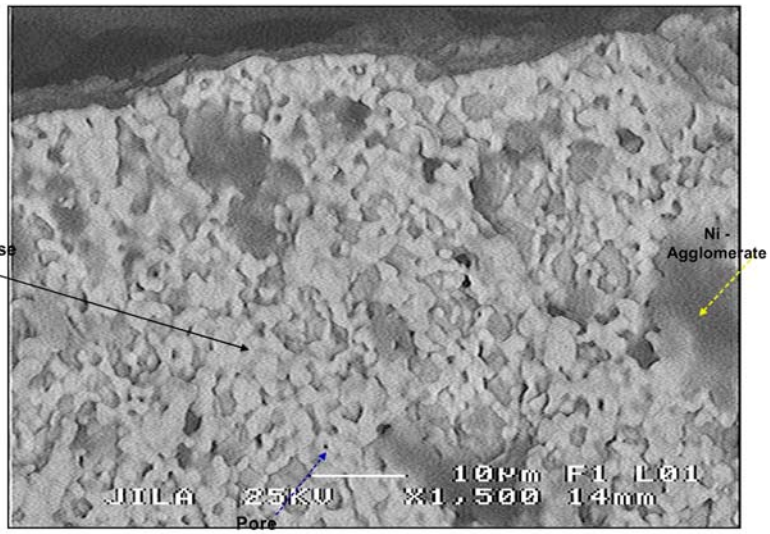

1-C). Back scattered image of phases

Figure 1 (A)–(F). SEM microstructures of dense 8 mole% Yittria Stabilized Zicronia and 25% porosity Ni–ZrO_2. (*Continued*.)

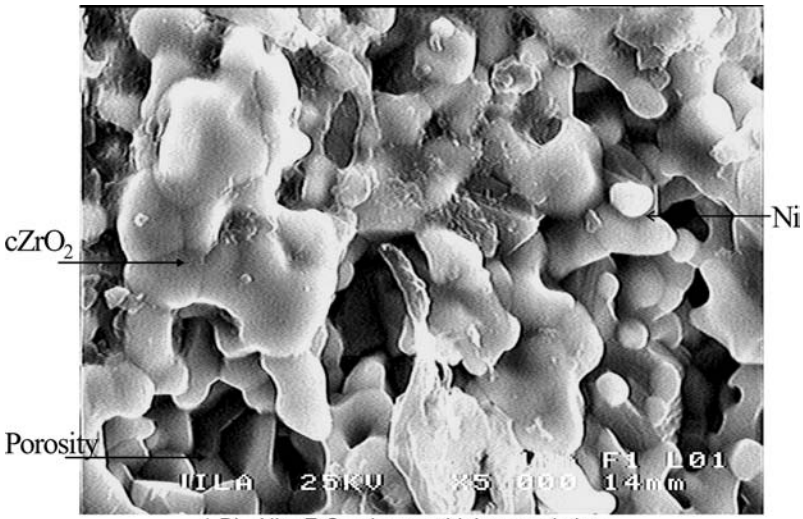

1-D). Ni-c-ZrO_2 phase at higher resolution.

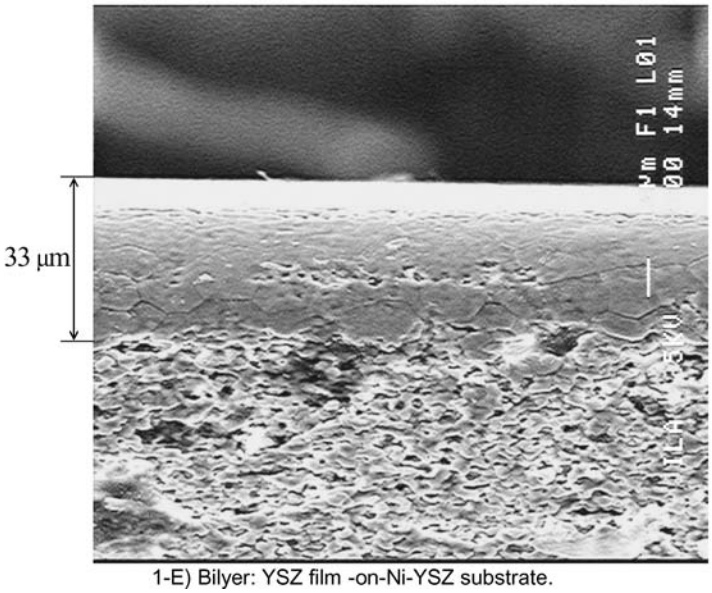

1-E) Bilyer: YSZ film -on-Ni-YSZ substrate.

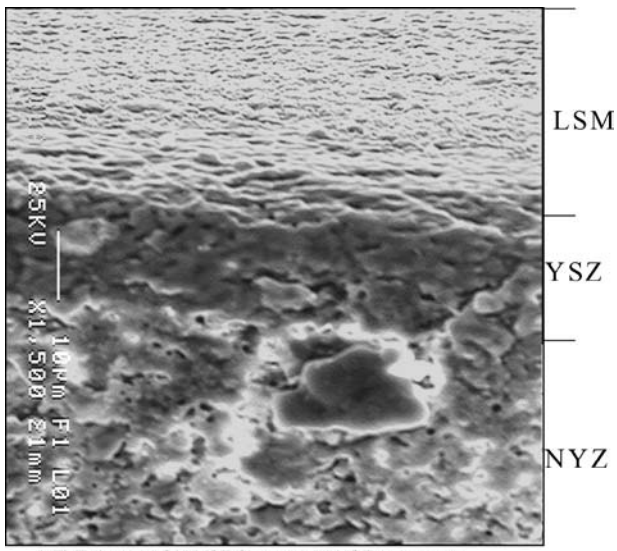

1-F) Trilayer: LSM/YSZ films-on-Ni-YSZ substrate.

Figure 1 (*Continued.*)

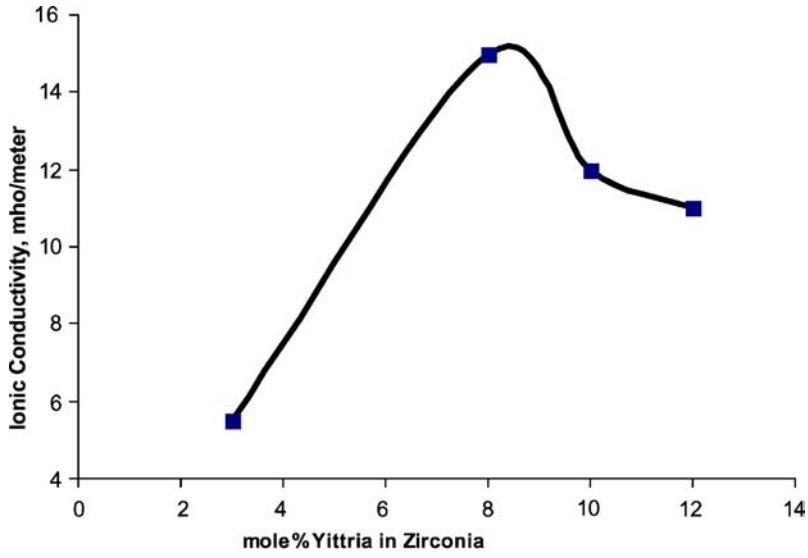

2-A) Ionic conductivity at 1000 °C (data after S.P.S Badwal et. al [27])

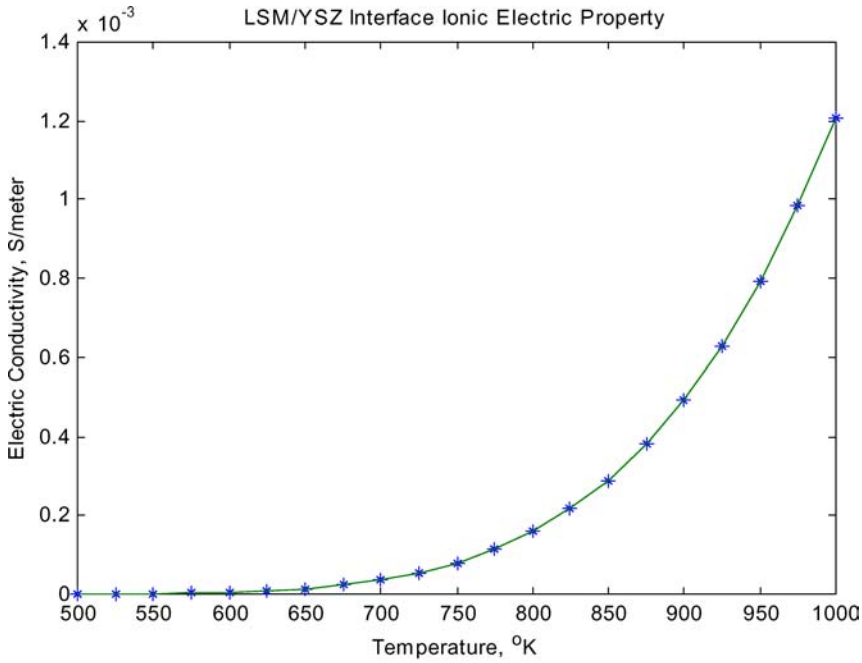

2-B). Ionic conductivity of the $La_2Zr_2O_7$ compounds formed at LSM/YSZ interface.

Figure 2 The ionic conductivity of Yittria Stabilzed Zirconia binary system and $La_2Zr_2O_7$ interface compound conductivity.

Average thermal strains accumulated in bulk materials over a range of temperatures can be estimated based on average coefficient of thermal expansion, CTE of YSZ using Equation (9b). Average CTE of the 8.1 mole% YSZ over temperature ranging from RT∼1000°C due to Kandil *et al*. [10], given in Equation (10) can be used to calculate the average thermal strains accumulated over a specified temperature range. The temperature dependant CTE represented by an *n*th degree polynomial in Equation (5) can be used to estimate the instantaneous thermal strains. The 6th order polynomial coefficients (Table I) for temperature dependent CTE (ppm/°K) of YSZ due to Sulec *et al*. [3], can be used to calculate the accumulated thermal strains at a given temperature. Residual thermal stress accumulated in the electrolyte made of YSZ due to thermal mismatch between CTEs of interconnect (α_{I}) and electrolyte (α_{e}) can be calculated by using a polynomial solution [18] for an integral given in Equation 12 based on average constant elastic modulus of electrolyte over a range of temperature extending from stress free ambient (T_{o}) to operating fuel cell temperature (T_{f}).

$$\alpha_{\mathrm{CTE}} f(T) = \sum_{i=0}^{n} a_i \cdot T^n \tag{11}$$

$$\sigma_{\mathrm{Residual}} = \int_{T_0}^{T_f} E_e \cdot (\alpha_I - \alpha_e) \cdot \Delta T \tag{12}$$

TABLE I Calculated coefficients of nth order polynomial for temperature dependent CTE (PPM/°C) of various fuel-cell materials

Coefficients	a_0	a_1	a_2	a_3	a_4	a_5	a_6
Materials							
8YSZ [3]	7.31E-06	−5.58E-09	6.54E-11	−1.57E-13	1.72E-16	−8.94E-20	1.79E-23
Ni-YSZ	8.223	0.0517	−2.00E-04	3.00E-07	−2.00E-10	6.00E-14	
Ni-ZrO_2	5.4113	0.0833	−0.3E-03	5.00E-07	−4.00E-10	1.00E-13	
E-Brite Interconnect	9.489	5.40E-03	6.00E-06	4.00E-09			

Residual thermal stress accumulating from RT (T_o=20°C) to operating temperature of a fuel-cells (T_f=800°C) in YSZ electrolyte for constant high temperature elastic modulus (E_e=155 GPa at 900°C) [3] but CTE varying with temperature up to 800°C, were used in the calculation. The super ferritic E-Brite interconnect with cubic polynomial function of CTE (Equation (11)) varying with temperature is used to predict thermal mismatch between electrolyte and interconnect materials. The residual stress in the electrolyte estimated from spread sheet calculations using Equation (13) was ∼220 MPa which was lesser than average flexural strength of 277 MPa for Ni-YSZ material determined by three-point bending test. This served as preliminary design stress in the fabrication of five layered unit stack of fuel cell assembly consisting of 60 unit stacks periodically repeating to achieve a target capability ∼1 KW of electricity.

4.1.2. Elastic properties of dense YSZ

The stiffness constants measured at Iowa State University by Kandil, Greiner and Smith [10] for 11–18 mole% Yittria doped Zirconia are used here to evaluate temperature dependent elastic bulk properties of Yittria Stabilized Zirconia from RT–800°C. Marked discrepancies in measured stiffness constants are noted from literature for 8 mole% Yittria stabilized Zirconia [8–10, 19–21]. At higher temperatures (300–500°C) measurement of ultrasonic wave propagation in longitudinal or transverse modes during thermal cycling of 8 mole% YSZ was highly unstable and inconsistent [10]. This could be attributed to the minimum dosage of Yittria (8 mole% Y_2O_3) required for cubic crystal stabilization of Zirconia seems to be unstable for achieving thermodynamic equilibrium at room temperature [10]. Anomalies can be confirmed from oscillatory trend of flexural strength of 8YSZ, reported by More *et al.* [22], which dropped significantly at 500°C from that at RT and then increased abruptly at 1000°C may be recalled here for the same thermodynamic instability. The isotropic bulk properties of elasticity of dense Yittria Stabilized Zirconia calculated from section 4.0 using the stiffness coefficients [10] are shown in Figs 3–5. Anisotropy factor of Yittria Stabilized Zirconia defined in Equation (6) clearly increases with molar concentration of Yittria but decreases with temperature for a given dosage of Yittria stabilizer over a range of 20–700°C. In other words, the isotropy of Zirconia increases with cubic stabilization by increasing dosage of Yittria (11–18 mole%). Effect of composition on the anisotropy factor of YSZ at 800°C can be defined by AF_{800}=0.0119 mole% Y_2O_3 + 0.206. Anisotropy factor of 8 mole% YSZ at 800°C is 0.3012 by extrapolation. At room temperature the anisotropy factor varied from 0.397–0.494 and extrapolated cubic spline fit values of anisotropy at 800°C varied from 0.341–0.413 with increasing composition of Yittria (11–18%). The Poisson's ratios of YSZ are determined by the ratio of compliance of -S_{12} to S_{11} [12]. Poisson's ratio of YSZ increases with composition of Yittria but not significantly affected by temperature up to 400°C. From 400–500°C, ratios seem to decrease and converge to fairly constant value thereafter at higher composition. A diverging trend for lower composition (at T>500°C) can't be explained (Fig. 3B). Thermodynamic instability of isotropic cubic YSZ structure for lower Yittria compositions of up to 12 mole% can be realized from lesser significance of Yittria dosage on Anisotropy factor (Fig. 3A). The effect is even more pronounced on the isotropic properties viz, Young's and Shear moduli in Fig. 4 and 5. The isotropic Young's modulus being independent of directional vector (R=0) can be determined from Equation 7 by inverse of S_{11}. The compositional dependence of Young's Modulus of YSZ containing up to 12 mole% Yittria is less significant and have E values ≥ 360 GPa at RT. Young's modulus decreases drastically with temperature by 25–30 GPa from RT to 700°C for YSZ containing Yittria up to 12 mole%. The isotropic Young's Moduli of YSZ have a maximum value at 12 mole% Yittria compositions over the entire temperature range from 20–800°C. The isotropic Young's modulus of YSZ decreases thereafter significantly by 25–30 GPa with Yittria composition ranging from 12–18 mole%. Similar trends are observed in Fig. 5, on the compositional and temperature dependence of isotropic Shear modulus of YSZ. The isotropic shear moduli are calculated from half of the inverse of difference in compliance between S_{11} and S_{12} [12]. Shear moduli are not significantly affected up to 12 mole% Yittria having G≥150 GPa at RT which drops by 10–15 GPa from RT to 800°C. The compositional dependence of shear modulus of YSZ also peaks at a maximum value 12.1%. The isotropic shear modulus decreases gradually with the composition (12–18 mol% Yittria) and linearly with temperature (20–800°C) by approximately 10 GPa. The bulk moduli of isotropic single crystal of YSZ can

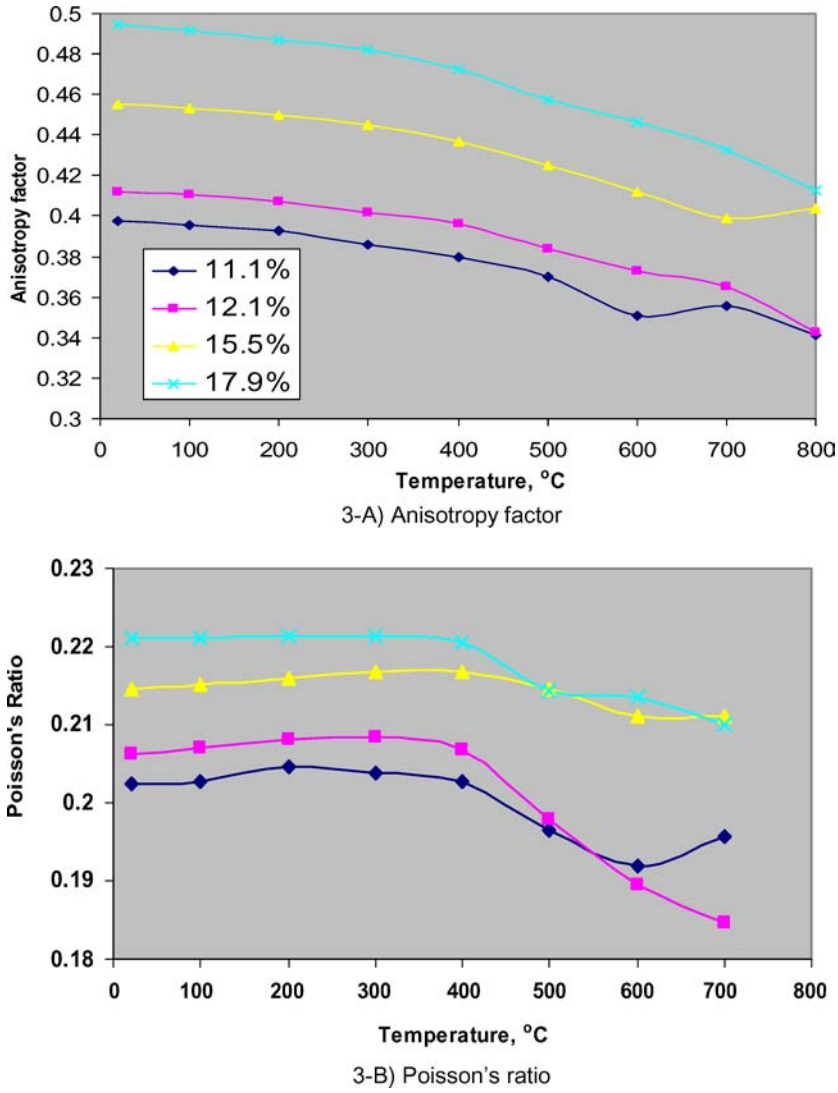

Figure 3 Anisotropy factor and Poisson's ratio varying with temperature and mole% of Yittria doped in Zirconia cubic single crystals

be calculated from one third of the inverse of sum compliance of S_{11} and $2S_{12}$. The cubic polycrystalline elastic moduli are identical to single crystal bulk moduli [10]. With the hypothesis that elastic moduli of polycrystalline cubic YSZ can be derived in terms of stiffness constants by the following relations (13a–c). The polycrystalline properties of various cubic crystal compositions of Yittria Stabilized Zirconia (11–18 mol% Yittria) at room temperatures (20°C) are tabulated (Table II). The polycrystalline Voigt bound average of Young's modulus of 88% c-ZrO_2 ($E_{100\%\,ZrO_2} = 220$ GPa) and that of 12% Y_2O_3 ($E_{100\%Y2O_3} = 175$ GPa) has an average Young's modulus of 215 GPa for 12 mole% YSZ which compares with predicted value of 205 GPa for the same within 5% error limit. The predicted elastic modulus for $E\langle 100\rangle$ of 12 mole% YSZ is 362 GPa in comparison with actual experimental E⟨100⟩ value of 370 GPa reported for 12 mole% YSZ [23]. The polycrystalline Young's moduli and Shear moduli indicate maximum elastic properties for 12 mole% YSZ until 400°C. By and large, polycrystalline properties decrease with composition above 12 mole% Yittria and temperatures (RT-800°C). However at temperatures above 400°C, polycrystalline properties of 15.5 mole% Yittria seem to dominate over those of 12 mole% Yittria Stabilized Zirconia.

TABLE II Polycrystalline properties of YSZ:.Elastic moduli (GPa) and Poisson's ratio

mol% Y_2O_3	$E_{YSZpoly}$	$G_{YSZpoly}$	$K_{YSZpoly}$	ν
		(a) T=20°C		
11.1	202.77	84.32	113.56	0.202412
12.1	205.23	85.07	116.47	0.206309
15.5	204.93	84.37	119.65	0.214540
17.9	204.00	83.53	121.89	0.221069
		(b) T=700°C		
11.1	176.73	73.90	96.82	0.19576
12.1	176.66	74.57	93.36	0.18462
15.5	184.27	76.08	106.25	0.21095
17.9	180.60	74.63	103.76	0.20992

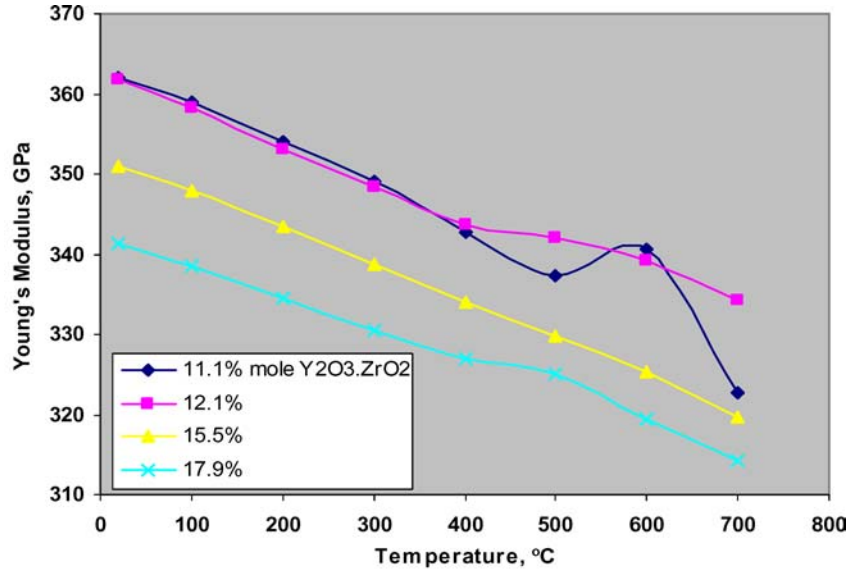

4-A) Young's moduli vs mole% Yittria and Temperature, °C

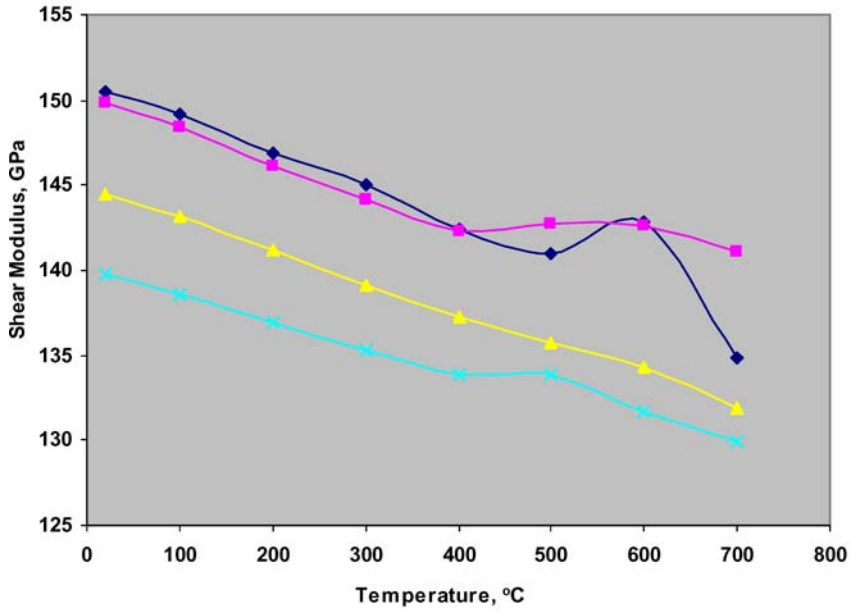

4-B) Shear moduli vs mole% Yittria and Temperaure, °C

Figure 4 Temperature dependence of Isotropic Young's modulus and Shear Moduli of Yittria doped Zirconia.

$$E_{\text{polycrystal}} \equiv K_{\text{sin glecrystal}} = \frac{(C_{11}+2C_{12})}{3} \tag{13a}$$

$$G_{\text{polycrystal}} = \frac{(C_{11}+C_{12})}{6} \tag{13b}$$

and

$$K_{\text{polycrystal}} = \frac{(C_{11}+2C_{12})(C_{11}+C_{12})}{9(C_{11}+C_{12})} \tag{13c}$$

On the basis of the isotropic Young's and Shear moduli as well as polycrystalline properties, it can be inferred that the 12 mole% Yittria Stabilized Zirconia is a better substitute for 8 mole% YSZ from the view point of structural, thermodynamic stability, improved isotropic elastic, thermo-elastic mechanical properties and strength required in fuel cell applications.

4.1.3. Porous Ni/YSZ

The microstructure of NiO-YSZ of sintered and reduced to Ni-YSZ is shown in Figure 1B–D, has average porosity of about 25%, being widely dispersed in the matrix. The NiO is reduced to bright shiny Ni particles or agglomerates are found scattered in the matrix of c-ZrO_2. The spherical Ni particles were seen in microstructure at higher magnification. At times the Ni was found surrounding the rim of pores in matrix. The SEM back scattered images con-

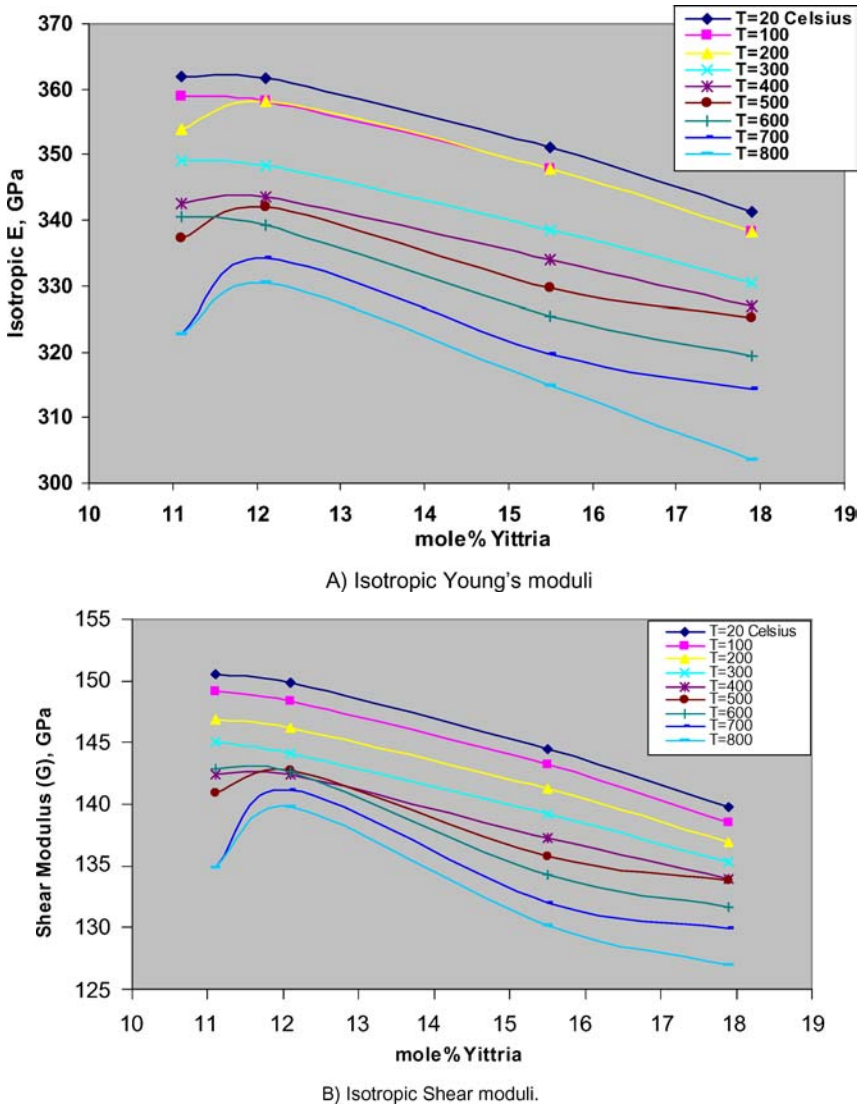

Figure 5 Determination of optimal composition of Yittria Stabilized Zirconia for improved thermo-elastic properties based on: A) Young's moduli and B) Shear moduli.

firmed the formation of Ni particles/agglomerates (grey) and cubic $Y_2O_3.ZrO_2$ dense (white) structures in reduced atmosphere. Average compositions of these structures were approximately YSZ $\sim$ 48%, Ni $\sim$ 27% and porosity $\sim$ 25%. The porosity manifested into a wide variety of crack morphology in the reduced Ni-YSZ microstructure. Typical types of crack morphology with their average size were circular (1–2 μm), elliptical (1$\times$3 μm), pinhole (0.5–1 μm), or slender slit (3–5 μm), type of porosity were delineated in reduced Ni-YSZ. However there were no channel or mud cracks [3, 6] seen at the interface of Bilayer (YSZ thin film on Ni-ZrO_2 substrate) or Trilayer (LSM/YSZ film on Ni-ZrO_2 substrate) structures (Fig. 1-E and 1-F). The multilayer films were intact and rigidly held on Ni-ZrO_2 substrate and were free from bending or warpage.

Average thermal expansion (CTE) of Ni/YSZ can be best described by the 5th order polynomial coefficients in Table 1 for Equation 12. A thermal mismatch due to CTE of the Dense YSZ and porous Ni-YSZ indicates that between the two (2–3 ppm/C) might result in thermal stress concentration at interface of anode/electrolyte. The excessive stress concentrations could cause delamination MEAs at the interface affecting overall functionality of fuel-cell [6, 7].

4.1.4. Elastic properties of Ni/YSZ

The porosity has a profound effect on the thermo-elastic properties of ceramic cermets. Even though the pores deteriorate the thermo-mechanical properties, porosity improves the electrical performance by ionic transport and thermal diffusivity by local convection of heat. Elastic properties of the porous Ni-YSZ substrates are determined based on elastic properties of the dense YSZ in the previous section. A simple form of Equation (14) can be used to correlate the Young's modulus of the dense and porous

materials of YSZ [24, 26, 27].

$$E_{\mathrm{NYZ}} = E_{ysz}\,(1 - b \cdot P) \tag{14}$$

where, P — %porosity in NYZ and b constant $\sim$ 3 for Zirconia based binary system. Young's modulus reduced Ni-YSZ with 25% porosity has E_{NYZ}=54 GPa using E_{YSZ}=204 [3, 6] for 8YSZ at the room temperature. Elastic modulus, E_{NYZ}=51 GPa closely conforms to the reported value of the NYZ E_{NYZ}=54 at RT [3, 6]. The Poisson's ratio of porous NYZ (μ_{NYZ}) relating to that of dense YSZ (μ_{YSZ}) with relatively pores free structure can be calculated using a relation between dense and porous ceramic materials due to Ramakrishnan and Arunachalam [28] in Equation (15): The Poisson's ratio of porous NYZ calculated using (16) and value of μ_{YSZ}=0.315 for dense YSZ is found to be μ_{NYZ}=0.2886 in comparison with reported value of 0.25 for the same at RT [3]. Thus it is possible to determine isotropic elastic properties porous of Ni-YSZ for various compositions (8–18 mole% YSZ) as a function of temperature (RT-800°C) using Equation 14 and 15.

$$\mu_{\mathrm{NYZ}} = 0.25\left(\frac{4\mu_{\mathrm{YSZ}} + 3P - 7\mu_{\mathrm{YSZ}} \cdot P}{1 + 2P - 3\mu_{\mathrm{YSZ}} \cdot P}\right) \tag{15}$$

5. Conclusion

Structure property correlation of dense and porous Yittria Stabilized Zirconia are established in order to investigate the impact of composition and temperature variation on thermo-elastic properties of isotropic single crystals and the polycrystalline properties. Anisotropy of the cubic structure is defined to understand the compositional variations in the dense YSZ. Elastic bulk properties are numerically predicted using the elastic stiffness constants reported in the literature. Thermo-elastic properties are evaluated for 8 mole% and 12 mole% Yittria Stabilized Zirconia. Effect of Yittria dosage in Zirconia on its lattice parameter, lattice constant, thermal diffusivity and ionic conductivity of the Yittria Stabilized Cubic Zirconia are investigated. A dosage of 8 or 9 mole% of Yittria in Zirconia seems to improve the ionic conductivity of the stabilized c-ZrO_2. The ionic conductivities of 8 and 12 mole% YSZ are not significantly altered at intermediate temperatures (600–800°K) however the former has slightly better ionic conductivities at higher temperatures. The ionic conductivity of $La_2Zr_2O_7$ type of compound formed in LSM/YSZ type of composite cathodes is found to be 1.2E-03 mho/meter at 1000°K. Even though a minimum of 8 mole% Yittria is necessary to retain the cubic crystal structure at room temperature in Zirconia based material it may be insufficient to achieve the thermal stability and thermo-dynamic equilibrium of Yittria Stabilized Zirconia. A numerical prediction of isotropic elastic properties have indirectly confirmed suspected susceptibility of 8 mole% Yittria Stabilized Zirconia to thermal and harmonic instabilities during thermal cycling.

Poisson's ratio increases with composition but remain constant up to a temperature 400°C. The compositional effect is not well defined at higher temperature. Poisson's ratio decreases with temperature from 400–800°C. Poisson's ratio of porous Ni-YSZ can be determined for any given temperature and composition from Equation (15). The isotropic elastic and shear Moduli increase with the composition of Yittria up to 12 mole% and decrease with any further increase of Yittria composition. Optimal isotropic elastic properties correspond to a composition of 12.1 mole% Yittria in cubic Zirconia. The directional dependence of single crystal elastic modulus for ⟨100⟩ orientation was found to be 362 GPa compared to experimental value of 370 GPa [23]. Elastic properties of porous Ni-YSZ can be determined from Equation 17 and elastic data of dense YSZ.

Acknowledgement

Authors are grateful for the financial support provided by NIST and ITN Energy Systems Inc. and the latter in particular for providing specimens for microscopic and mechanical testing. Author (SPG) thanks David Alchen (JILA, Physics Dept.,) for helping him in SEM work and Gregory Forsha, (ME department) at CU-Boulder for experimental work respectively.

References

1. W. A. MEULENBERG, O. TELLER, U. FLESCH, H. P. BUCHKREMER and D. STOVER, *J. Mater. Sci.* **36** (13) (2001) 3189..
2. R. WILKENHOENER, H. P. BUCHKREMER, D. STOLTEN and A. KOCH, *ibid* **36** (2001) 1775.
3. A. SELUC and A. ATKINSON, *ibid.* **36** (2001) 1173.
4. A. SELUC and A. ATKINSON, *J. Am. Ceram. Soc.* **83** (2000) 2029.
5. S. PRIMDAHL, B.F. SORENSON and M. MOGENSEN, *ibid.* **83** (2000) 489.
6. B.F. SORENSON and S. PRIMDAHL, *ibid.* **33** (1998) 5291.
7. N. Q. MINH, *ibid.* **76** (3) (1993) 563.
8. N. G. PACE, G. A. SAUNDERS, Z. SUMENGEN and J. S. THORP, *ibid.* **4** (12) (1969) 1106.
9. J. D. BUCKLEY and D. N. BRASKI, *ibid.* **50** (4) (1967) 220.
10. H. K. KANDIL, J. D. GREINER and J. F. SMITH, *ibid.* **67** (5) (1984) 220.
11. SHIVA GADAG, GANESH SUBBARAYAN andWILLIAM BARKER, Fractography of Monolithic and Multilayer Films on NiO/YSZ Substrates Used in Fuel Cells Applications.∗Paper in submission.
12. R. F. COOK and G. M. PHARR: Mechanical Properties of Ceramics in Structure and Properties of Ceramics, edited by R. W. Cahn, P. Haasen and E. Kramer, Materials Science and Technology, V11 by M. Swain, Chapter 7 (VCH Publishers Inc. printed in NY, USA 1994), p 3414.
13. Mechanical Behavior of Materials, Vol. I: Elasticity and Plasticity, edited by D. Francois, A. Pineau and A. Zaoui (Kluwer Academic, The Netherlands, 1998).
14. Structural residual stress analysis by nondestructive methods, edited by V. Hauk (Elsevier, The Netherlands, 1997).

15. S. P. S. BADWAL, Ceramic Superionic Conductors in Structure and Properties of Ceramics, edited by R.W. Cahn, P. Haasen, E. Kramer, Materials Science and Technology, V11 by M. Swain, Chapter 11 (VCH Publishers Inc. printed in FRG 1994), p 568.
16. S. P. S. BADWAL and F. T. CIACCHI, *Key Engng. Mater.* **V48-50** (1990) 235.
17. V. I. ALEKSANDROV, G. E. VAL'YANO, B. V. LUKIN, V. V. OSIKO, A. E. RAUTBORT, V. M. TATARINTSEV and V. N. FILATOV, *Izv. Akad. Nauk SSSR, Neorg. Mater*. 12(2) (1976) 273.
18. SHIVA GADAG and GANESH SUBBARAYAN: "Thermomechanical Analysis of Sequential Stack of Solid Oxide Fuel Cells (PSOFC)". Paper in preparation.
19. R. N. THURSTON, *Proc., IEEE* **53** (1965)1320.
20. M. FARLEY, J. S. THORP, J. S. ROSS and G. A. SAUNDERS, *J. Mater. Sci. Lett*. **7** (4) (1972) 475.
21. T. HAILING and G. A. SAUNDERS, *ibid.* **1** (9) (1982)416.
22. M. MORE, T. ABE, H. ITOH, O. YAMAMATHO, Y. TAKEDA and T. KAWAHARA, *Solid State Ionics* **74** (1994) 157.
23. F. J. RITZERERT, H. M. YURI and R. V. MINER, *J. Mater. Sci*. **33** (1998) 5339.
24. CAHN, HAASEN and KRAMER: Structure and Properties of Ceramics, edited by R.W. Cahn, P. Haasen, E. Kramer, Materials Science and Technology, V11 by M. Swain, Chapter 11, VCH Publishers Inc. printed in FRG (1994), p568.
25. D. MUNZ and T. FETT (Eds.), "Ceramics", Springer-verlag, (1999).
26. R.W. RICE, (Ed.), "Porosity of Cermics", Marcel Dekker, Inc., 1998.
27. T. E. MATIKAS, P. KARPUR and S. SHAMASUNDER, *J. Mater. Sci*. **32** (4) (1997) 1093.
28. N. RAMAKRISHNAN and V. S. ARUNACHALAM, *ibid.* **25** (1990) 3930.

Received 11 August 2004
and accepted 7 June 2005